Two-Dimensional Microwave Imaging Approach Based on a Genetic Algorithm

Salvatore Caorsi, *Member, IEEE* and Matteo Pastorino, *Senior Member, IEEE*

***Abstract*—In this paper, a multi-illumination multiview approach to microwave imaging is proposed, which is based on a genetic algorithm (GA). The inverse problem is recast in an optimization problem, solved in the framework of the Born approximation. The formulation of the approach is described and images of reconstructed circular (multilayer) cylinders are reported.**

***Index Terms*—Born approximation, genetic algorithms, microwave imaging.**

I. Method Formulation and Imaging Configuration

In the present paper, we propose a microwave imaging (MI) approach for reconstructing unknown cylindrical dielectric objects under TM illumination (TM_z) conditions. The starting point for MI approaches in the spatial domain is the Fredholm integral equation, which relates the scattered electric field $\mathbf{E}^{\mathrm{scat}}(\mathbf{r})$ (measured in a suitable domain D) to the internal field $\mathbf{E}^{\mathrm{tot}}(\mathbf{r})$ and to the dielectric properties of the scatterer [1]–[3]:

$$\int_A \tau(\mathbf{u}) E^{\mathrm{tot}}(\mathbf{u}) \Gamma(\mathbf{x}/\mathbf{u})\, d\mathbf{u} - E^{\mathrm{scatt}}(\mathbf{x}) = 0 \quad \mathbf{x} \in D(\not\subset A) \tag{1}$$

where only the z components of the field vectors are involved and $\mathbf{x} = (x, y)$. In relation (1), A denotes the test area (containing the scatterer cross section); $\Gamma(\mathbf{x}/\mathbf{u})$ is the two-dimensional (2-D) Green's function for free-space; finally, $\tau(\mathbf{x})$ is the *object function* given by $\tau(\mathbf{x}) = k_0^{-2}[k_A^2(\mathbf{x}) - k_0^2]$, where $k_A(\mathbf{x})$, and k_0 denote the wavenumbers in region A and in the external medium, respectively.

In this paper, we exploit a stochastic technique for global optimization, which is based on a genetic algorithm (GA) [4]–[6]. Although stochastic optimizers, when they are implemented on serial computers, are slow in comparison with more standard techniques (like the distorted Born iterative method (DBIM) [7]), GA's exhibit several interesting features: 1) they have been found to be very robust in terms of capability to reach global minima [4]; 2) it is possible to insert a lot of *a priori* information into the solving procedure; 3) they allow a natural implementation on parallel computers that it seems to be the only possible way of managing a lot of data in a reasonable time. For example, a GA has been recently applied for imaging of perfectly conducting objects [8].

Manuscript received September 30, 1997; revised October 29, 1999.

S. Caorsi is with the Department of Electronics, University of Pavia, Pavia, I-27100 Italy.

M. Pastorino is with the Department of Biophysical and Electronic Engineering, University of Genoa, Genova, I-16145 Italy.

Publisher Item Identifier S 0018-926X(00)02453-4.

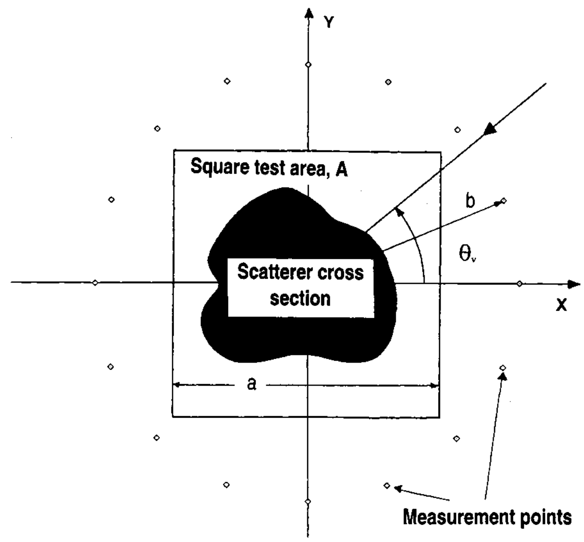

Fig. 1. Imaging configuration.

The proposed approach to MI is studied here in the framework of the first order Born approximation (BA) [1], which increases the speed of the optimization. The BA acts a linearization of (1) and is valid only for weakly scattering objects. However, in conjunction with the GA, the approach turned out to be rather efficient and some interesting reconstructions have been obtained.

As an imaging configuration (Fig. 1), we assumed a square test area (side: $a \times a$) and an observation domain made of P measurement points, equally spaced on an arc of circumference of radius b. A set of V incident TM_z plane waves is assumed whose propagation directions are defined by the angles $\vartheta_v = (v-1)(2\pi/V), v = 1, \cdots, V$. A multi-illumination multiview approach is considered in which the observation domain jointly rotate with the illuminating source. After linearization by the BA for which $|E^{\mathrm{scat}}(\mathbf{x})| \ll |E^{\mathrm{inc}}(\mathbf{x})|, \mathbf{x} \in A$, the following *fitness function* (FF) (acting on discrete unknowns) can be defined in (2), shown at the bottom of the next page, where N is the number of subdomains, τ_n is the (constant) value of the object function inside the nth subdomain, $\mathbf{x}_{jp}$ denotes the pth measurement point for the jth view, and $\gamma(\mathbf{x}_{jp}/\mathbf{x}_n)$ indicates the integral of the Green function performed over the nth subdomain and calculated at point $\mathbf{x}_{jp}$. The minimization of the FF is obtained by a GA [4]–[6], which is based on a random search of the (global) minimum. In the *initialization* phase, a set of M trial solutions is randomly generated. It constitutes a *population* of *chromosomes*, which are arrays given by $T_m = [\tau_{1m}\tau_{2m} \cdots \tau_{Nm}]$, $m = 1, \cdots, M, \tau_{nm}$ being the value of the object function inside the nth subdomain of A. Each τ_{nm} value

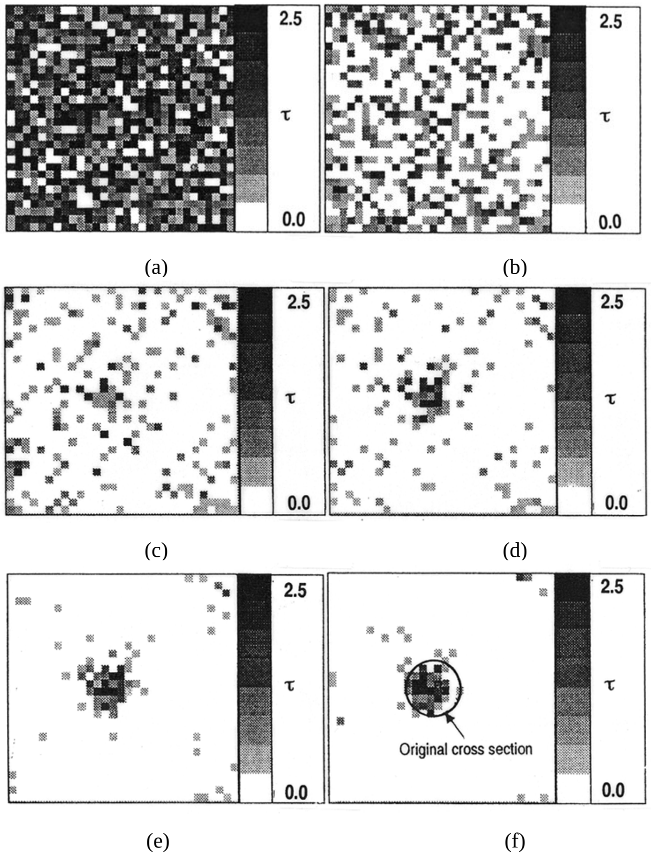

Fig. 2. Reconstruction of a lossless homogeneous cylinder (first example). Object function at different iterations. k: iteration number. (a) $k = 1$ (initialization step). (b) $k = 200$. (c) $k = 600$. (d) $k = 800$. (e) $k = 1000$. (f) $k = 2000$.

is selected in the range $0.0 \leq \tau_{nm} \leq \tau_{nm}^{*}$, $m = 1, \cdots, M$, $n = 1, \cdots, N, \tau_{nm}^{*}$ being given by $\tau_{nm}^{*} = K\tau(\mathbf{x}_n)$, where $\tau(\mathbf{x}_n)$ is the value of the original object function at $\mathbf{x}_n$ and K is a given constant. This represent a way to introduce some *a priori* information on the object since the choice of K limits the search space for the solution of the optimization process. In particular, if K is correctly fixed (according to the available *a priori* information), not realistic values of τ_{nm} can be avoided.

Moreover, each chromosome T_m is encoded in a binary sequence Λ_m (*binary chromosome*) by means of a Q-level quantizer. At this point the iterative process starts and the population at a generic step $k+1$ (the population dimension, M, is kept unchanged) is computed on the basis of the population at step k by using the genetic operators of selection, crossover, and mutation [4]–[6]. The iterative process continues until a stopping criterion is satisfied ($F\{\tau_1, \tau_2, \cdots, \tau_N\} \leq F_{\text{th}}$, F_{th} being a fixed threshold) or a given number of iterations is completed.

TABLE I
DIELECTRIC RECONSTRUCTIONS
(FIGS. 2 AND 3).

Σ_o: PERCENTAGE MEAN ERRORS ON THE RECONSTRUCTION OF THE OBJECTS. Σ_b: PERCENTAGE MEAN ERRORS ON THE RECONSTRUCTION OF THE BACKGROUND. $\tau_{\max}$: MAXIMUM VALUE OF THE RECONSTRUCTED OBJECT FUNCTION

Number of views	Σ_b	Σ_o	τ_{max}
Single homogeneous cylinder (Figure 2)			
V = 4	0.9 %	18.2 %	1.81
Hollow cylinder (Figure 3)			
V = 1	7.85 %	42.6 %	1.98
V = 2	5.92 %	21.1 %	1.96
V = 3	5.52 %	19.8 %	1.88
V = 4	5.38 %	19.8 %	1.87

II. NUMERICAL RESULTS

In the first example, the scattering object is a homogeneous circular cylinder. The assumed parameters are the following: diameter $d = \lambda_o/4$, (λ_o, free-space wavelength); $\tau = 1.0$; $a = \lambda_o$; $N = 900$ (discretization cells); $V = 4$ (unit uniform plane waves); $P = 32$ (measurement points), $b = 1.5\lambda_o$ (diameter of the observation domain). For this canonical scatterer, the values of the scattered electric field on the measurement points have been computed by using the analytical solution in terms of Bessel eigenfunctions. The other data concerning the GA (chosen according to values suggested in the literature) are the following: population dimension, $M = 100$; probability of crossover, $P_c = 0.7$; probability of mutation, $P_m = 0.0004$; number of quantization levels, $Q = 256$; constant value for the searching range definition, $K = 5$. Fig. 2 gives reconstructed images of the test area. At the initialization step $(k = 1)$, completely random values are assumed. When the number of iterations increases, the background becomes more and more clear and the location of the scatterer very accurate. At step $k = 2000$, the reconstruction seems rather good. The quantitative reconstruction errors are expressed through the following parameters (given in Table I): the percentage mean errors on the reconstruction of the scatterer (Σ_o) and of the background (Σ_b); maximum value of the reconstructed object function $(\tau_{\max})$. For this example, some further investigations with different values of M, P_c, and P_m have been performed. It resulted that, although the computational load notably increases, the reconstruction quality does not improve significantly for $M > 100$. For example, we obtained $\Sigma_o \approx 0.8\%$ and $\Sigma_b \approx 16\%$ for

$$F\{\tau_1, \tau_2, \cdots, \tau_N\} = \left| \sum_{j=1}^{V} \sum_{p=1}^{P} E^{\text{scat}}(\mathbf{x}_{jp}) - \sum_{n=1}^{N} \tau_n E^{\text{inc}}(\mathbf{x}_n) \gamma(\mathbf{x}_{jp}/\mathbf{x}_n) \right|^2 \tag{2}$$

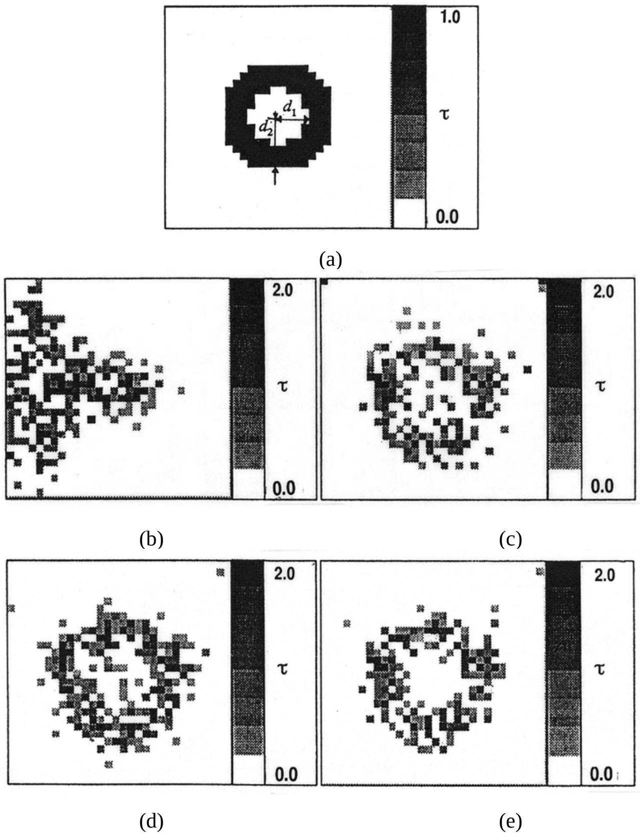

Fig. 3. Reconstruction of a hollow cylinder (second example) Object function for different numbers of views (V). (a) Actual object (discretized); (b) $V = 1$ (single view process). (c) $V = 2$. (d) $V = 3$. (e) $V = 4$.

$M = 120$ and $\Sigma_o \approx 0.7\%$ and $\Sigma_b \approx 14.5\%$ for $M = 200$. On the contrary, if M decreases, the quantitative errors become large ($\Sigma_b \approx 23\%$ and $\Sigma_b \approx 65\%$ for $M = 80$ and $M = 40$, respectively). Concerning the effects of P_c, we have found that $\Sigma_o < 1.2\%$ and $\Sigma_b < 25\%$ for $0.6 < P_c < 0.8$, but large errors have been obtained for lower values of this probability (e.g., $\Sigma_b > 40\%$ for $P_c < 0.5$). Finally, for this example, P_m must be kept small, as the quantitative errors sharply increase when P_m increases (e.g., $\Sigma_b > 48\%$ for $P_m > 0.0008$ and $\Sigma_b > 75\%$ for $P_m > 0.001$). These results confirm, at least for the present case, the validity of the values suggested in the literature on the subject [5], [6]. The above results have been obtained in about 4.5-min CPU time on a PC Pentium using a nonoptimized code, with a memory requirement of about $MN \times 16$ bytes.

In the second example, a hollow cylinder has been considered. The internal and external radii are given by $d_1 = \lambda_o/4$ and $d_2 = \lambda_o/2$, respectively. The object function is given by $\tau = 1.0$. The same square investigation domain ($N = 900$ subdomains) was used and the same parameters for the GA were considered. Even in this case, the values of the scattered electric field in the observation domain have been analytically computed.

Fig. 3 shows the original (discretized) cross section of the cylinder and the reconstruction images. Table I gives the quantitative errors. As expected, the single-view process $(V = 1)$ is unable to reconstruct such a rather complex scatterer, but for $V = 3$ and $V = 4$, the location is very good, very limited spatial noise is present in the background and also the shape of the cylinder is retrieved in a quite acceptable way, considering that the reconstruction is performed within the Born approximation.

III. Conclusion

In this paper, an approach to 2-D microwave imaging has been proposed that is based on a GA. The method is applied in the framework of the first-order Born approximation, which results in a quadratic fitness function. Although better results can be obtained by using more complex approaches (like the distorted Born iterative method [8]) or more sophisticated fitness functions, the presented results seem unusually accurate for being obtained by using this simplified scheme. A version of the approach able to take into account the nonlinear form of the inverse scattering equations for strong scatterers is currently under development.

References

[1] T. M. Habashy, M. L. Oristaglio, and A. T. de Hoop, "Simultaneous nonlinear reconstruction of two-dimensional permittivity and conductivity," *Radio Sci.*, vol. 29, pp. 1101–1118, 1994.

[2] T. Melamed and E. Heyman, "Spectral analysis of time domain diffraction tomography," *Radio Sci.*, vol. 32, pp. 593–603, Mar.–Apr. 1997.

[3] N. Joachimowicz, C. Pichot, and J.-P. Hugonin, "Inverse scattering: An iterative numerical method for electromagnetic imaging," *IEEE Trans. Antennas Propagat.*, vol. 39, pp. 1742–1752, Dec. 1991.

[4] D. E. Goldberg, *Genetic Algorithms in Search, Optimization, and Machine Learning*. Reading, MA: Addison-Wesley, 1989.

[5] R. L. Haupt, "An introduction to genetic algorithms for electromagnetics," *IEEE Antennas Propagat. Mag.*, vol. 37, pp. 7–15, Apr. 1995.

[6] D. S. Weile and E. Michielssen, "Genetic algorithm optimization applied to electromagnetics: A review," *IEEE Trans. Antennas Propagat*, vol. 45, pp. 343–353, Mar. 1997.

[7] W. C. Chew and Y. M. Yang, "Reconstruction of two-dimensional permittivity distribution using the distorted Born iterative method," *IEEE Trans. Med. Imag.*, vol. 9, pp. 218–225, 1990.

[8] C.-C. Chiu and P.-T. Liu, "Image reconstruction of a perfectly conducting cylinder by the genetic algorithm," *Proc. Inst. Elect. Eng.*, pt. H, vol. 143, pp. 249–253, June 1996.

Salvatore Caorsi (M'99) received the Laurea degree in electronic engineering from the University of Genoa, Italy, in 1973.

Since 1994, he has been a Full Professor of electromagnetic compatibility at the Department of Electronics, University of Pavia, Italy. His primary activities focus in applications of electromagnetic field to telecommunications, artificial vision and remote sensing, biology, and medicine. In particular, he is working on research project concerning human hazard to electromagnetic exposure, numerical methods for solving electromagnetic problems, wave interaction in the presence of nonlinear media, inverse scattering and microwave imaging, and electromagnetic compatibililty.

Prof. Caorsi is the past president and founding member of the Inter-University Research Center for the Interactions Between Electromagnetic Fields and Biological Systems (ICEmB). He is a member of the Elettrotecnica ed Elettronica Italiana (AEI), the European Bioelectromagnetic Association (EBEA), and the European Society for Hyperthermic Oncology (ESHO).

Matteo Pastorino (M'90–SM'96) received the Laurea (electronic engineering) and Ph.D. (electronics and computer science) degrees from the University of Genoa, Genoa, Italy, in 1987 and 1992, respectively.

Currently, he is an Associate Professor of Electromagnetic Fields at the Department of Biophysical and Electronic Engineering, University of Genoa, Italy, where he is responsible for the Applied Electromagnetics Group. He teaches university courses in electromagnetic fields and remote sensing and electromagnetic diagnostics. His main research interests are in the field of electromagnetic direct and inverse scattering, microwave imaging, wave propagation in presence of nonlinear media, and analytical and numerical methods in electromagnetism.

Dr. Pastorino is member of the IEEE Instrumentation and Measurement Technical Committee on Imaging Systems, the Associazione Elettrotecnica ed Elettronica Italiana (AEI), and the European Bioelectromagnetic Association (EBEA).